Biosensors and Bioelectronics 35 (2012) 200–205

Contents lists available at SciVerse ScienceDirect

Biosensors and Bioelectronics

journal homepage: www.elsevier.com/locate/bios

Real-time analysis of the carbohydrates on cell surfaces using a QCM biosensor: a lectin-based approach

Zhichao Pei[a,b,*,1], Julien Saint-Guirons[b,1], Camilla Käck[b], Björn Ingemarsson[b], Teodor Aastrup[b]

[a] State Key Laboratory of Crop Stress Biology in Arid Areas and College of Science, Northwest A&F University, Yangling, Shaanxi 712100, People's Republic of China
[b] Attana, SE-11419 Stockholm, Sweden

ARTICLE INFO

Article history:
Received 4 January 2012
Received in revised form 19 February 2012
Accepted 20 February 2012
Available online 28 February 2012

Keywords:
QCM biosensor
Mammalian cells
Lectins
Kinetics
Glycosylation

ABSTRACT

A novel approach to the study of molecular interactions on the surface of mammalian cells using a QCM biosensor was developed. For this study, an epidermoid carcinoma cell line (A-431) and a breast adenocarcinoma cell line (MDA-MB-468) were immobilized onto polystyrene-coated quartz crystals. The binding and dissociation between the lectin Con A and the cells as well as the inhibition of the binding by monosaccharides were monitored in real time and provided an insight into the complex avidic recognition of cell glycoconjugates. The real-time lectin screening of a range of lectins, including Con A, DBA, PNA and UEA-I, enabled the accurate study of the glycosylation changes between cells, such as changes associated with cancer progression and development. Furthermore, the kinetic parameters of the interaction of Con A with MDA-MB-468 cells were studied. This application provides investigators in the field of glycobiology with a novel tool to study cell surface glycosylation and may also have impacts on drug discovery.

1. Introduction

In this post-genomic era, the interest in glycomics has greatly increased because the oligosaccharide chains of many glycoproteins appear to be involved in a variety of biological functions, including blood clotting, structural support, hormone activation and recognition, the storage of bioactive molecules, cell migration and cell–cell and cell–matrix interactions and adhesion (Springer, 1990; Varki, 1993). In particular, plasma membrane proteins serve mainly as enzymes, channels or cell/protein receptors, and most of these proteins undergo glycosylation as they traffic through the secretory pathway. Glycans confer additional properties such as shape, hydrophobicity and charge, and they may interact with carbohydrate-binding proteins. There is a considerable body of evidence detailing the abnormal glycosylation of glycoproteins in cancer development. The changes in the carbohydrate composition of cancer cells have been shown to play a critical role in the cell–cell and cell–matrix interactions necessary for cancer cell survival, invasion and metastasis. For instance, when cells are oncogenically transformed, they often express fetal carbohydrates called oncofetal antigens. A variety of oncofetal changes in cancer glycosylation have been described, including an increased N-linked carbohydrate size due to extensive branching, the increased expression of the Lewis sugars and the truncation of carbohydrates such as those observed on mucin-type glycoconjugates, which exposes structures such as the T and Tn antigens (Dwek and Brooks, 2004). Several findings have led to an interest in lectins with respect to cancer research, particularly the ability of some lectins to bind preferentially to malignant cells (reviewed in Sharon and Lis, 2004).

Lectins are carbohydrate-binding proteins of non-immune origin that agglutinate cells or precipitate glycoconjugates. Lectins were first identified in the 19th century by Peter Herman Stillmark (1888), who described a protein extract from the seeds of the castor tree (*Ricinus communis*) that had hemagglutinin activity, i.e., the extract could agglutinate erythrocytes (Franz, 1988). Lectins have played a crucial role in determining the sugar composition of antigens associated with the ABO blood group system as well as in the observation of the glycans exposed at the surface of mammalian cells (Morgan and Watkins, 2000). Although new techniques to study complex carbohydrates have emerged, such as mass spectrometry (Mutenda and Matthiesen, 2007), the use of lectins remains a method of choice to study the role of carbohydrates in numerous biological systems, especially glycosylation changes occurring at the surface of mammalian cells that lead to the development of diseases such as cancer and metastasis. In addition, lectins have been studied as diagnostic tools and therapeutic agents in cancer research (Grossbard et al., 1998; Multani et al., 1998).

* Corresponding author at: State Key Laboratory of Crop Stress Biology in Arid Areas and College of Science, Northwest A&F University, Yangling, Shaanxi 712100, People's Republic of China. Tel.: +86 29 87080351; fax: +86 29 87080351.
E-mail addresses: zhichao.pei@attana.com, peizhichao18@yahoo.com (Z. Pei).
[1] These authors contributed equally to this work.

0956-5663/$ – see front matter © 2012 Elsevier B.V. All rights reserved.
doi:10.1016/j.bios.2012.02.047

Biosensors based on the quartz crystal microbalance (QCM) technology have proved to be a powerful and efficient tool to study molecular interactions, particularly antigen–antibody interactions (Koutsopoulos et al., 2009; Pei et al., 2010; Dahlbäck et al., 2011). However, QCM technology has also been used to study lectin–carbohydrate recognition (Pei et al., 2005). In this study, we present a new approach that combines the use of lectins and a QCM biosensor to analyze lectin–carbohydrate interactions occurring at the surface of immobilized cancer cells. This method enabled the first analysis of cell carbohydrates using label-free lectins under dynamic conditions. This analysis led to the direct evaluation of both quantitative and qualitative parameters, such as the binding intensity, the inhibition potential of monosaccharides and the kinetic parameters, providing insight into the nature of glycoconjugates exposed at the cell surface. Previous work using QCM biosensors and mammalian cells has been performed with an emphasis on monitoring morphological changes (Marx et al., 2007; Tan et al., 2008). However, our method fixed the cells to rigidify the surface and enable both the qualitative and quantitative evaluation of the binding events occurring at the surface of cancerous cell lines (A-431, MDA-MB-468). In this work, the jack bean lectin concanavalin A (Con A) was used as a typical lectin because it has widely been studied (Lis and Sharon, 1998) and has been used in QCM biosensor studies on immobilized polysaccharides (Pei et al., 2005). Other lectins, such as *Dolichos biflorus* agglutinin (DBA), peanut agglutinin (PNA) and *Ulex europaeus* agglutinin I (UEA-I), were used to further corroborate our findings.

First, we demonstrated the ability of this new method to specifically and reproducibly monitor the binding events that occur between a lectin (Con A) and cancer cells (A-431) immobilized on the surface of a quartz crystal in real time. We also demonstrated the ability of such cell crystals to be regenerated, thus enabling the measurement of several binding events on the same cells. This crucial aspect of the method enabled the study of lectin–cell interactions with a high degree of reproducibility. We also showed that the QCM technology was suitable for real time quantitative/qualitative lectin screening. In addition, the method that we developed enabled us to screen for potential inhibitors (carbohydrates) and provided insight into the binding mechanism of lectins to cancer cells by determining the rate constants.

2. Experimental

2.1. Chemicals and reagents

Methyl α-D-mannopyranoside, methyl α-D-glucopyranoside, concanavalin A (Con A), fluorescein isothiocyanate-conjugated concanavalin A (FITC-Con A), *Dolichos biflorus* agglutinin (DBA), peanut agglutinin (PNA) and *Ulex europaeus* agglutinin I (UEA-I) were purchased from Vector Laboratories. The blue nucleic acid stain DAPI (4′,6-diamidino-2-phenylindole, dihydrochloride) was purchased from Invitrogen. All other reagents were purchased from Sigma.

2.2. Cell culture

The human epidermoid carcinoma cell line A-431 (ATCC: CRL-1555) and the mammary gland adenocarcinoma cell line MDA-MB-468 (ATCC: HTB-132) were grown in 75 cm^3 flasks (Sarstedt) and maintained in Dulbecco's modified Eagle's medium (DMEM, GIBCO) supplemented with 10% (v/v) heat-inactivated fetal bovine serum (GIBCO) and 0.1% (v/v) penicillin/streptomycin (GIBCO). All the cell lines were grown at 37 °C with 5% CO_2 and 95% humidity (MiniGalaxy, LabRum, Klimat) and were maintained by changing the medium every 2 days and passaging every 5–days using standard trypsinization protocols.

2.3. Preparation of cell crystals

An AT cut, gold-plated 10 MHz quartz crystal was spin-coated with polystyrene (0.5% solution in toluene) to an average thickness of 56 Å ± 21 Å. Further UV treatment was performed to increase the wettability of the surface (Zhang et al., 2000). A-431 or MDA-MB-468 cells were grown for 24 h on the polystyrene-coated quartz crystal. The subsequent fixation was performed using standard formaldehyde-based procedures. The cell-crystals were visualized under a microscope (Nikon Eclipse 80i) after the nuclei were stained with DAPI according to the manufacturer's recommendations. The cell-crystals were then stored in PBS at 4 °C before being placed in a chip holder and inserted into an Attana Cell A100 QCM biosensor (Attana AB, Stockholm, Sweden). The cell-crystals were robust and could be stored in PBS at 4 °C for several weeks before use.

2.4. QCM analysis of lectin–cell interactions

All the lectin-binding experiments were performed with an Attana Cell A100 QCM biosensor designed to enable the analysis of cell–lectin interactions. The running buffer consisted of 10 mM phosphate buffered saline (pH 7.4) supplemented with 0.025% Tween (PBST), and a continuous flow of 25 μL/min was maintained throughout. The resonant frequency of the quartz crystal and the frequency shift (d*F*) associated with binding events or dissociation were recorded with the Attester software (Attana AB, Stockholm, Sweden). A 50 μL injection loop was used, and only 37 μL was injected to diminish dispersion. The lectin samples and the corresponding controls were prepared in running buffer. The binding events were monitored for 84 s. After injection, the dissociation of the lectins was monitored for at least 300 s, unless stated otherwise. The bound lectins were desorbed between measurements by repeatedly (2–4 injections) injecting a regeneration solution consisting of 10 mM glycin (pH 1.0) with 0.5 M NaCl. The life-time of cell crystal is dependent on the cell type and the subsequent regeneration conditions used. Here, each cell crystal has been used to record about 10 binding cycle (association–dissociation–regeneration) in average.

For the inhibition studies, methyl α-D-mannopyranoside, methyl α-D-glucopyranoside and D-galactose were preincubated for 20 min with Con A. A reference solution consisting of running buffer supplemented with the appropriate amount of monosaccharide was injected prior to each measurement.

2.5. Microscopic evaluation of lectin–cell binding

The cell nuclei (counterstained with diamidino-2-phenylindole, DAPI, ex/em: 345 nm/458 nm) and the lectin Con A (labeled with fluorescein isothiocyanate [FITC], ex/em: 488 nm/520 nm) were observed directly at the sensor surface using a fluorescent microscope (Nikon Eclipse 80i). This approach was used to confirm the specificity of the interaction between Con A and A-431 cells monitored by the QCM biosensor.

2.6. Estimation of K_D

The simple exponential responses from the binding of Con A to the surface carbohydrates of cancer cells were determined using the Attana Cell A100 system associated with the Attester software (Attana AB, Stockholm, Sweden). The data were then analyzed using the biosensor kinetic data analysis software ClampXP developed by Myszka and Morton (1998). This program interprets the

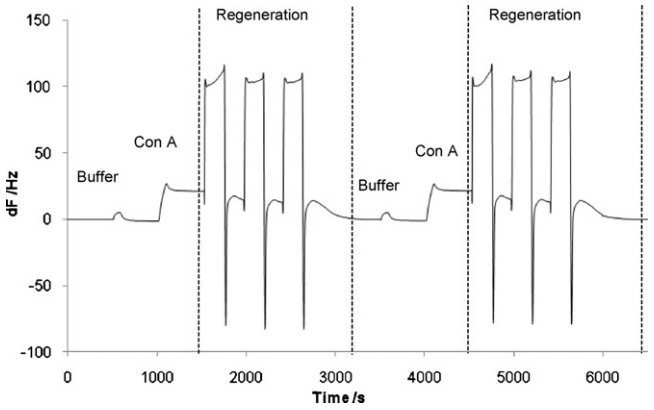

Fig. 1. Binding of FITC-Con A (0.24 μM) to immobilized A-431 cells. Frequency shift (dF) was recorded during the association (84 s) and dissociation (400 s) phases of the interactions between FITC-Con A and A-431 cells, and subsequent release of the remaining bound Con A by injection of the acid solution (glycin 10 mM, pH 1.0, NaCl 0.5 M). The A-431 cell surface was completely regenerated after three successive injections of the acid solution.

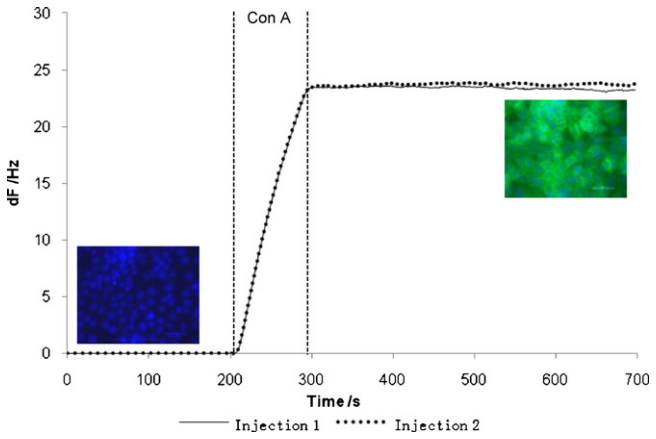

Fig. 2. Reproducibility and specificity of the binding of FITC-Con A to A-431 cells. Two binding curves obtained successively with regeneration in between, were superimposed (solid and dotted lines). Fluorescent images of both nuclei (in blue) and FITC-Con A (in green) were taken before (left handside) and after (right handside) injection of FITC-Con A. (For interpretation of the references to color in this figure legend, the reader is referred to the web version of the article.)

kinetics of a reaction by fitting theoretical models based on hypothetical mechanisms. The data sets were overlaid with the fit of a 1:1 interaction model (with or without a mass transport limitation) to evaluate how well the rate constants described the interaction of interest. The fitted data sets were used to extract estimates of the binding constants, such as the association rate (k_a), the dissociation rate (k_d) and the resulting dissociation constant (K_D), which characterize the affinity of the interaction of interest.

3. Results

3.1. QCM measurements

The cell-crystals, consisting of A-431 cells immobilized on the surface of polystyrene-coated quartz crystals, were placed in an Attana Cell A100 QCM biosensor and equilibrated under a continuous flow (50 μL/min) of running buffer. The equilibration step usually took place overnight, as the process may require several hours. The measurements were initiated when the resonant frequency was stable (baseline drift <0.2 Hz/min). When the cell-crystal oscillated at a stable resonant frequency, several reference injections consisting of running buffer, were performed to assess the surface prior to the evaluation of the interactions between the lectins and cell surface glycans. Fig. 1 shows a typical experiment in which two injections of FITC-Con A at 0.24 μM (used in this experiment to enable a fluorescent evaluation of the binding) were performed successively with regeneration steps in between. The running buffer was injected over the surface as a reference before every injection of the lectin. Typically, lectin or buffer was injected for 84 s, which corresponded to the injection of 75% of the volume contained in the injection loop in an attempt to minimize dispersion.

All the measurements were performed at a flow rate of 25 μL/min, and the injections of analytes were performed as follows. The association phase was monitored for 84 s and was followed by a 300 s wash phase, during which dissociation occurred. The remaining bound lectin was desorbed by injecting a low pH regeneration solution. The surface was regenerated when all of the remaining bound lectin had been desorbed from the surface. On the sensorgram, the regeneration was monitored in real time and was complete when the frequency was stable and identical to the frequency recorded before the injection of FITC-Con A. The surface could then be used to evaluate another lectin–cell interaction. The responses of the cell-crystals to replicate injections of FITC-Con A were extracted from the sensorgram and analyzed using the Attester software (Attana AB, Stockholm, Sweden) and ClampXP (Myszka and Morton, 1998) to determine the binding constants. Both the association and dissociation phases of the interaction between FITC-Con A and A-431 cells were evaluated in duplicate and are shown in Fig. 2. The signal increased as FITC-Con A bound to the glycoconjugates exposed at the surface of A-431 cells, and it did not decay exponentially, suggesting that the interaction might be limited by mass transport. The maximal recorded frequency shift (dF_{max} = 23 Hz) and the association (k_a) and dissociation (k_d) rate constants were similar for both measurements ($k_{a1} = 3.6 \times 10^5\ M^{-1}\ s^{-1}$, $k_{a2} = 5.2 \times 10^5\ M^{-1}\ s^{-1}$; $k_{d1} = 6 \times 10^{-5}\ s^{-1}$, $k_{d2} = 3.2 \times 10^{-5}\ s^{-1}$). The binding responses of the two replicate injections of FITC-Con A were reproducible. This result confirmed that the regeneration of the cell-crystals performed between two successive injections was effective and enabled the reproducible evaluation of several binding events on the same surface. Furthermore, a microscopic evaluation of the above-mentioned interaction was performed before and after the injection of the lectin. Both cell nuclei (DAPI, shown in blue in Fig. 2) and lectins (FITC-Con A, shown in green in Fig. 2) were observed before and after injection of FITC-Con A. Before injection, only cell nuclei were observed, confirming the presence of cells on the surface. The fluorescent evaluation performed after the interaction between the lectin and the cells had been monitored with the biosensor showed a mainly peripheral localization of the lectin (in green, Fig. 2). These observations indicated that the frequency shift monitored on the sensorgram specifically reflected the interactions occurring at the surface of the A-431 cells between Con A and membrane glycoconjugates.

3.2. Maximal frequency shift and cell coverage

An experiment was designed to further confirm the specificity of the interaction between Con A and A-431 cells. Several surfaces were prepared with a varying amount of immobilized A-431 cells, expressed as a percentage of the surface coverage. The response at the end of the injection phase (dF_{max}) was plotted against cell density (Fig. 3). In this experiment, Con A at 0.24 μM and surfaces of varying cell density, ranging from 0% (no cells) to 80% cell coverage (as visually determined by microscopy), were used. There was an exponential increase in the dF_{max} with the cell coverage of the crystal. This result confirmed the specificity of the binding event monitored by the QCM biosensor. It is also important

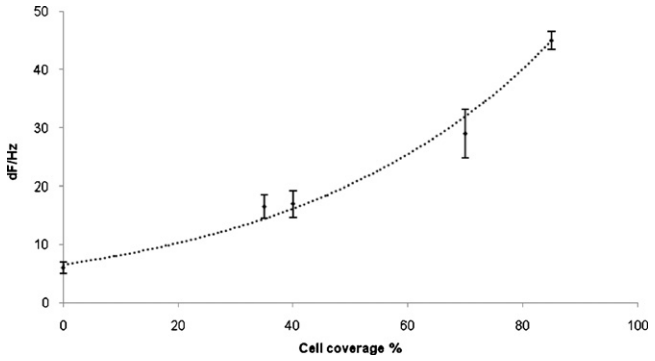

Fig. 3. Maximal frequency shift (dF_{max}) and cell coverage. Crystals with a varying amount of immobilized A-431 cells (from 0% to 80% coverage) were used. Injections of Con A at 0.24 μM were performed on each surface and the frequency shift was recorded and plotted (mean ± SEM).

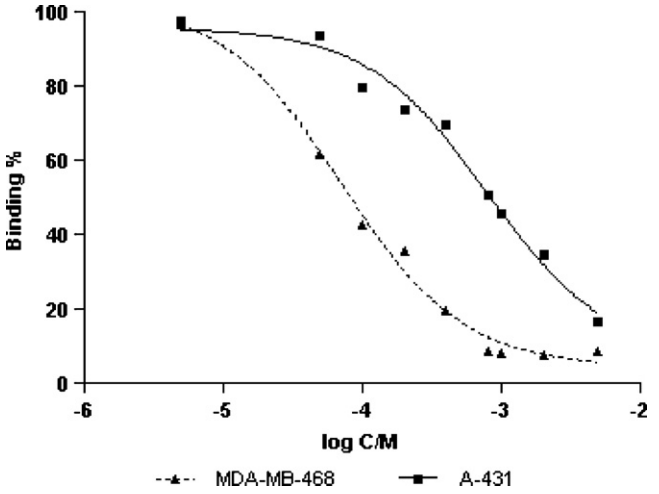

Fig. 4. Competition Plots of α-D-mannopyranoside: Inhibition of the interaction of Con A (0.24 μM) with MDA-MB-468 and A-431 cells using methyl α-D-mannopyranoside.

to note that the interactions between Con A and the cell-free surface reached a maximal value of approximately 6 Hz. It is essential to bear in mind that those interactions probably occurred between Con A and the fetal bovine serum (GIBCO) glycoproteins adsorbed on the crystal surface. The 6 Hz value was maximal on cell-free crystal and would be less important when cells covered up to 60% of the surface, making serum glycoproteins less accessible for interaction with Con A. This experiment also indicates that minor changes in the sensor surface cell coverage may induce major differences in the intensity of the response recorded. Therefore, it is important to perform several experiments on the same surface for comparison with regeneration between the experiments.

3.3. Competitive inhibition of the lectin binding

Con A can interact with monosaccharides, such as D-mannopyranoside and D-glucopyranoside, and has an especially strong affinity for methyl α-D-mannopyranoside (Pei et al., 2005). In mammalian cells, Con A recognizes complex structures, such as the outer trimannosyl group of high mannose and bisected hybrid type glycopeptides, suggesting the multivalent binding of Con A to cells (Bhattacharyya et al., 1987; Branderhorst et al., 2008). Cell-crystals that were 50–80% covered with immobilized MDA-MB-468 cells were used. Our biosensor-based approach was used for the evaluation of the inhibition of lectin–cell binding by monosaccharides. To this end, Con A was incubated with a soluble inhibitor such as methyl α-D-mannopyranoside, methyl α-D-glucopyranoside or the irrelevant carbohydrate D-galactose. The binding of Con A with or without an increasing amount of a competing or non-binding monosaccharide was measured using the Attana Cell A100 QCM biosensor; regeneration was performed in between each measurement. The responses were monitored, and the binding curves of Con A alone and in the presence of methyl α-D-mannopyranoside (5 μM–1 mM) are shown as an example (Fig. S1.A in supplementary information). The competition plots obtained for each studied carbohydrate (methyl α-D-mannopyranoside, methyl α-D-glucopyranoside and D-galactose) are displayed in Fig. S1.B (in supplementary information). D-galactose (50 μM–1 mM) presented little inhibition, confirming its lack of inhibition of Con A binding, while both methyl α-D-mannopyranoside and methyl α-D-glucopyranoside appeared to specifically inhibit the interaction of Con A with MDA-MB-468 cells. Methyl α-D-mannopyranoside proved to be a better inhibitor than methyl α-D-glucopyranoside; 87 μM and 0.34 mM of these monosaccharides, respectively, were needed to reduce the maximal response measured for the binding of Con A (0.24 μM) to MDA-MB-468 cells by half.

Furthermore, a competition assay with methyl α-D-mannopyranoside was performed on MDA-MD-468 and A-431 cell-crystals of similar cell densities. The concentrations of methyl α-D-mannopyranoside needed to inhibit 50% of the binding of Con A to MDA-MB-468 and A-431 cells were 87 μM and 0.89 mM, respectively (Fig. 4). The multi-specificity of Con A (Branderhorst et al., 2008) could explain this discrepancy, and it seems that the specificity and affinity of the Con A–cell interaction were greatly driven by the composition of the cell surface carbohydrates. Indeed, the complexity of the surface and its multivalency has been demonstrated to greatly influence the interaction of cells with lectins, including Con A. Pei et al. (2006) and Branderhorst et al. (2008) have studied the interactions of Con A with multivalent and monovalent surfaces, respectively. These studies have shown that the half-maximal effective concentration (EC_{50}) of methyl α-D-mannopyranoside increased with the valency of the surface. Our work also demonstrated that this technique enabled us to measure complex binding events, such as lectin–cell interaction.

3.4. Saturation of cell surface

Saturation occurs when the binding sites on the surface are fully occupied; the intensity of the response at saturation is the maximum frequency, R_{max}. Saturation experiments determine the surface capacity and the stoichiometry of the studied interaction (Rich and Myszka, 2008). Con A was injected over an A-431 cell crystal at concentrations ranging from 48 nM to 48 μM. The responses were subsequently monitored and are shown in Fig. S2 (in supplementary information).

3.5. Lectin screening

A range of lectins, including Con A, DBA, PNA and UEA-I, was injected over A-431, MDA-MB-468 and cell-free crystals. The lectin screening, which consisted of sequential injections of lectins separated by regeneration steps, was performed on the same surface, which allowed for the reproducibility and significance of the results. The above-mentioned lectins were injected over either A-431, MDA-MB-468 or cell-free surfaces at 0.48 μM. The responses were subsequently monitored by the Attana Cell A100 QCM biosensor, and the maximum frequency shift (dF_{max}) obtained for each lectin was recorded and summarized in Table 1.

Table 1
Lectin Screening: Con A, DBA, PNA, SBA and UEA-I were injected over three different surfaces, where two surfaces consisted of immobilized cells (A-431 and MDA-MB-468 cells) and one reference surface without any cells. The maximum frequency shift (dF_{max}) obtained for each lectin was recorded and summarized.

Lectins	dF_{max} (Hz)		
	A-431	MDA-MB-468	No cells
Con A	150	27	7.5
DBA	35	0	0
PNA	0	0	0
SBA	45	0	0
UEA-I	8	0	0

The mannose-binding lectin Con A exhibited some binding to the cell-free crystal (dF_{max} = 7.5 Hz), high binding to the MDA-MB-468 crystal (dF_{max} = 27 Hz) and very high binding to the A-431 crystal (ΔF_{max} = 150 Hz). This result could be explained by the preferential binding of Con A to the highly branched glycoconjugates on the surface of A-431 cells. The binding frequencies of DBA, SBA and UEA-I were also recorded with maximum frequency shifts of 35 Hz, 45 Hz and 8 Hz, respectively, on the A-431 cell crystal, but no responses could be measured on the MDA-MB-468 and cell-free crystals (Fig. S3, in supplementary information). PNA did not interact with any of the three surfaces used in this experiment (Fig. S3). These results suggested that A-431 and MDA-MB-468 cells expressed different levels of N-acetyl-glucosamine-, D-glucose- and mannose-containing glycoconjugates on their surfaces. Similar to the cell-based fluorescent assay, these quantitative measurements highlighted the differential expression of glycoconjugates on the surface of mammalian cells (A-431 and MDA-MB-468 in this study). In addition, the real-time measurement of the responses obtained for each of the lectins enabled a qualitative analysis of the lectin–cell interaction. This information might complement the interpretation of the data by providing insights into the attachment of these lectins to cellular glycoconjugates. For instance, the interaction profiles of SBA, DBA, UEA-I and PNA with A-431 presented varying maximum frequency shifts, but they all exhibited rapid dissociation behavior (50% of bound lectins dissociated within 2 min), as opposed to the stable binding observed with Con A (Fig. S2). This result suggested that the real-time measurement of rapidly dissociating lectins in particular could be more accurate than a classical cell-based microtiter plate assay in which the extent of lectin–cell interactions could be underestimated due to the delayed measurement and extensive wash steps.

3.6. Estimation of the kinetic parameters of the interaction of Con A with MDA-MB-468 cells

The interactions between Con A and immobilized MDA-MB-468 cells were evaluated using the Attana Cell A100 QCM biosensor. Briefly, MDA-MB-468 crystals were prepared as described in the experimental section. The analyte (Con A) was then injected over the surface, and the measured responses are presented in Fig. 5 along with the theoretical 1:1 fit produced by the ClampXP software. The immobilization of the cells on the sensor surface is expected to affect the amount of accessible targets on the cell surface for the low expression level targets. However, in this experiment, the targets on cell surface are abundant carbohydrates to the binding lectin and therefore the immobilization level on the sensor surface did not perturb the kinetic results compared with the free cells if a 1:1 interaction model used. Although the data and fits do not overlay exactly because of the complexity of the data, we can estimate the binding constant of the interaction of Con A with MDA-MB-468 cells with confidence. The magnitude of the K_D of this interaction was low

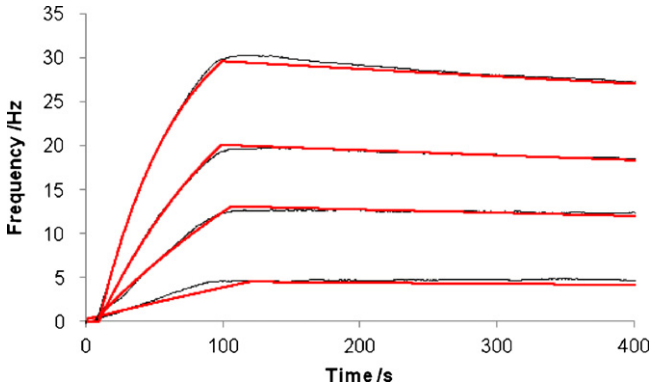

Fig. 5. Kinetic evaluation of the interactions between Con A and immobilized MDA-MB-468 cells. Con A at 0.12–0.96 μM was injected and the responses were recorded (black lines). Theoritical 1:1 fit generated by the ClampX software were overlaid (red lines). The association and dissociation constant (k_a = 19856 M^{-1} s^{-1}; k_d = 3.02 × 10^{-4} s^{-1}) as well as the affinity constant (K_D = 16 nM) were obtained. (For interpretation of the references to color in this figure legend, the reader is referred to the web version of the article.)

(K_D = 15 nM) compared to the reported K_D measured with monovalent mannose derivatives (K_D = 100 μM). As previously mentioned, the multivalency associated with the complexity and heterogeneity of the glycoconjugates exposed at the cell surface as well as the oligomerization of lectins (Shinohara et al., 1997) and receptor clustering (Monsigny et al., 2000) may explain this discrepancy, although the latter is quite unlikely due to the fixation of the cells.

4. Discussion

QCM biosensors have been successfully used to study antibody–antigen interactions (Koutsopoulos et al., 2009) and have proven to be valuable tools to evaluate lectin–carbohydrate interactions (Pei et al., 2005) and lectin–bacteria interactions (Hong et al., 2009) and for studying the effects of drugs on human cells (Marx et al., 2007; Tan et al., 2008). However, a novel approach was needed to monitor lectin–mammalian cell interactions in real time. We have developed a method based on the immobilization of human cancerous cell lines onto polystyrene-coated quartz crystals that enabled a qualitative and quantitative evaluation of the interactions occurring at the cell surface between glycoconjugates and carbohydrate-binding proteins (lectins). Although the formaldehyde-based fixation impact on the recognition of the cells compared with the intact cells due to cell surface protein cross-linking, in our experiment, the fixation method used is to study the carbohydrates on the cell surface. The use of polystyrene has been shown to be compatible with QCM measurements and has several advantages, as it mimics the surface used in cell-based microtiter plate assays (Kase et al., 1999). The viscoelastic properties of the cells were modified by a fixation method to fall within the scope of application of Sauerbrey's equation, which links the monitored frequency change to the mass added to the crystal surface (Sauerbrey, 1959). The cell immobilization process was monitored using a nuclear dye and fluorescent microscopy. Crystals with between 50% and 80% of the surface covered by cells were chosen to provide the optimal signal/load ratio. Indeed, the load of the crystal, as measured by the quality factor (Q), varies with the number and type of cells. The oscillator used in the Attana Cell A 100 QCM biosensor has the ability to drive crystals with Q values >500, and the cell coverage of 50–80% was measured to be above that threshold for all the cell lines used in this study. The above-mentioned conditions enabled us to produce cell-crystals suitable for the real-time analysis of lectin–cell interactions. Both the association and dissociation

phases recorded for replicate injections of Con A were superimposable, indicating the high reproducibility and robustness of our measurements. The initial binding rate and the rate of the dissociation phase appeared linear, instead of exponential, suggesting that the binding rate of the analyte was faster than its diffusion rate to the surface (mass transport limitation). The method that we developed enabled us to evaluate the potential for carbohydrates that bound specifically or non-specifically to Con A to inhibit the binding of this lectin to cell surfaces. It appeared, as previously reported by other investigators (Branderhorst et al., 2008), that the structure and composition of cellular glycoconjugates played a crucial role in their interactions with Con A. For instance, the different mannose contents of the two cancer cell lines investigated (A-431 and MDA-MB-468) were clearly apparent, as the concentration of methyl α-D-mannopyranoside needed to inhibit 50% of the binding of Con A was 10-fold higher for the A-431 cells than for the MDA-MB-468 cells. The combination of lectin screening and inhibition experiments using glycopeptides or synthetic polysaccharides may provide investigators with an additional tool to unravel the complex glycosylation changes that occur during the development of cancer. This novel method fills a gap between classic real-time biosensor using the purified receptor (which cannot reflect the complex cell environment) and cell based assay/flow cytometry (which cannot obtain the full kinetics of biomolecule interactions).

5. Conclusion

In this study, we have described a method based on the use of a QCM biosensor that permits the evaluation of molecular interactions at the surface of mammalian cells. We showed that the QCM technology was suitable for real-time, label-free measurements of the interactions between lectins and membrane glycoconjugates in a cellular environment, thereby conferring a higher biological relevance to the data. The key feature of this method lies in the regeneration of the cells (desorption of bound analyte) after an interaction has been monitored. This regeneration has enabled us to measure several binding events using the same immobilized cells. Real-time lectin screening generated both qualitative and quantitative data, offering a subsequent advantage over an enzyme-linked lectin assay (ELLA). This new biosensor-based method could also be used to screen for lectin inhibitors to better understand lectin-binding mechanisms and to study the cell surface carbohydrate composition.

Acknowledgment

This work was supported by the European Commission (contract no. MRTN-CT-2006-019561).

Appendix A. Supplementary data

Supplementary data associated with this article can be found, in the online version, at doi:10.1016/j.bios.2012.02.047.

References

Bhattacharyya, L., Haraldsson, M., Brewer, C.F., 1987. J. Biol. Chem. 262 (3), 1294–1299.
Branderhorst, H.M., Ruijtenbeek, R., Liskamp, R.M., Pieters, R.J., 2008. Chembiochem 9 (11), 1836–1844.
Dahlbäck, M., Jørgensen, L.M., Nielsen, M.A., Clausen, T.M., Ditlev, S.B., Resende, M., Pinto, V.V., Arnot, D.E., Theander, T.G., Salanti, A., 2011. J. Biol. Chem. 286 (18), 15908–15917.
Dwek, M.V., Brooks, S.A., 2004. Curr. Cancer Drug Targets 4 (5), 425–442.
Franz, H., 1988. Adv. Lectin Res. 1, 10–25.
Grossbard, M.L., Fidias, P., Kinsella, J., O'Toole, J., Lambert, J.M., Blattler, W.A., Esseltine, D., Braman, G., Nadler, L.M., Anderson, K.C., 1998. Br. J. Haematol. 102 (2), 509–515.
Hong, S.R., Choi, S.J., Jeong, H.D., Hong, S., 2009. Biosens. Bioelectron. 24 (6), 1635–1640.
Kase, T., Suzuki, Y., Kawai, T., Sakamoto, T., Ohtani, K., Eda, S., Maeda, A., Okuno, Y., Kurimura, T., Wakamiya, N., 1999. Immunology 97 (3), 385–392.
Koutsopoulos, S., Unsworth, L.D., Nagai, Y., Zhang, S., 2009. Proc. Natl. Acad. Sci. U.S.A. 106 (12), 4623–4628.
Lis, H., Sharon, N., 1998. Chem. Rev. 98 (2), 637–674.
Marx, K.A., Zhou, T., Montrone, A., McIntosh, D., Braunhut, S.J., 2007. Anal. Biochem. 361 (1), 77–92.
Monsigny, M., Mayer, R., Roche, A.C., 2000. Carbohydr. Lett. 4, 35–42.
Morgan, W.T., Watkins, W.M., 2000. Glycoconj. J. 17 (7-9), 501–530.
Multani, P.S., O'Day, S., Nadler, L.M., Grossbard, M.L., 1998. Clin. Cancer Res. 4 (11), 2599–2604.
Mutenda, K.E., Matthiesen, R., 2007. Methods Mol. Biol. 367, 289–301.
Myszka, D.G., Morton, T.A., 1998. Trends Biochem. Sci. 23 (4), 149–150.
Pei, Z., Anderson, H., Aastrup, T., Ramström, O., 2005. Biosens. Bioelectron. 21, 60–66.
Pei, Z., Anderson, H., Myrskog, A., Dunér, G., Ingemarsson, B., Aastrup, T., 2010. Anal. Biochem. 398, 161–168.
Pei, Z., Larsson, R., Aastrup, T., Anderson, H., Lehn, J-M., Ramström, O., 2006. Biosens. Bioelectron. 22, 42–48.
Rich, R.L., Myszka, D.G., 2008. J. Mol. Recognit 21 (6), 355–400.
Sauerbrey, G., 1959. Z. Phys. 155, 206–222.
Sharon, N., Lis, H., 2004. Glycobiology 14 (11), 53R–62R.
Shinohara, Y., Hasegawa, Y., Kaku, H., Shibuya, N., 1997. Glycobiology 7 (8), 1201–1208.
Springer, T.A., 1990. Nature 346, 425–434.
Tan, L., Jia, X., Jiang, X., Zhang, Y., Tang, H., Yao, S., Xie, Q., 2008. Anal. Biochem. 383, 130–136.
Varki, A., 1993. Glycobiology 3 (2), 97–130.
Zhang, D., Dougal, S.M., Yeganeh, M.S., 2000. Langmuir 16 (10), 4528–4532.